

Superconductivity Centennial Conference

Main Design Principles of the Cold Beam Pipe in the Fast Ramped Superconducting Accelerator Magnets for Heavy Ion Synchrotron SIS100

A. Mierau^a, P. Schnizer^b, E. Fischer^b, J. Macavei^b, S. Wilfert^b, S. Koch^a,
T. Weiland^a, R. Kurnishov^c, P. Shcherbakov^d

^a*Institut Theorie Elektromagnetischer Felder, Technische Universität Darmstadt, Schlossgartenstraße 8, Darmstadt 64289, Germany*

^b*GSI Helmholtzzentrum für Schwerionenforschung GmbH, Planckstraße 1, Darmstadt 64291, Germany*

^c*Electroplant, Moscow, Russia*

^d*IHEP - Protvino, Protvino 142281, Moscow Region, Russia*

Abstract

SIS100, the world second large scale heavy ion synchrotron using fast ramped superconducting magnets, is to be built at FAIR. Its high current operation of intermediate charge state ions requires stable vacuum pressures $< 10^{-12}$ mbar under dynamic machine conditions which are only achievable when the whole beam pipe is used as an huge cryopump. In order to find technological feasible design solutions, three opposite requirements have to be met: minimum magnetic field distortion caused by AC losses, mechanical stability and low and stable wall temperatures of the beam pipe. We present the possible design versions of the beam pipe for the high current curved dipole. The pros and cons of these proposed designs were studied using simplified analytical models, FEM calculations and tests on models.

© 2012 Published by Elsevier B.V. Selection and/or peer-review under responsibility of the Guest Editors.

Open access under [CC BY-NC-ND license](#).

Keywords: superconducting magnets, cryogenic vacuum chamber, magnetic field computation, thermal analysis, thin metal sheets

1. Introduction

The heavy ion synchrotron SIS100, to be built at FAIR (Facility for Antiproton and Ion Research near by Darmstadt, Germany), will be the world's second fast ramped synchrotron using superconducting magnets. The high current operation of intermediate charge state ions U^{28+} is limited by the time one has to keep the ions at low energy and by the ultra-high vacuum (UHV). These two requests lead to a fast ramped machine design with a maximum field strength of 1.9 T for a dipole field, a cycle frequency of 1 Hz and an average vacuum pressure in the range of 10^{-12} mbar within the beam pipe. Further the field homogeneity within the pipe was specified to be 600 ppm. All these conditions brought up the final design of the machine: superconducting magnets of the Nuclotron type [1] and a cold beam pipe, operated below 15 K to provide the required vacuum quality [2].

Due to the fast field variation, eddy current effects will be rather intense in the SIS100 dipole chambers. This leads to a unwanted heating up of the chamber walls. In order to keep the heat load for the cryogenic

system at an acceptable level, the wall thickness of the dipole vacuum chambers is limited to 0.3 mm only. This low thickness, in turn, requires a proper stabilisation of the thin-walled vacuum chamber.

According to the first design issue the vacuum chamber consisting of the beam pipe and the support ribs is cooled by a two phase forced helium within its own cooling circuit. The cooling tubes are welded to the chamber (see Fig. 1), whereby they form an electrical loop which affects the achievable field homogeneity [3]. Therefore an alternative design is investigated now [4], which is based on a proper thermal contact

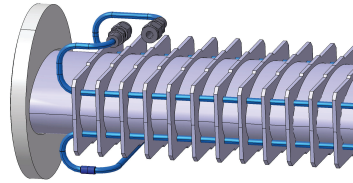


Fig. 1. The vacuum chamber with an additional cooling circuit. In this approach the cooling tubes are welded on the ribs.

between the cold magnet yoke and the vacuum chamber (see Fig. 2). The new design is studied using analytical approximations and numerical models for estimating the mechanical stability as well as the heat conduction power and the expected field distortions.

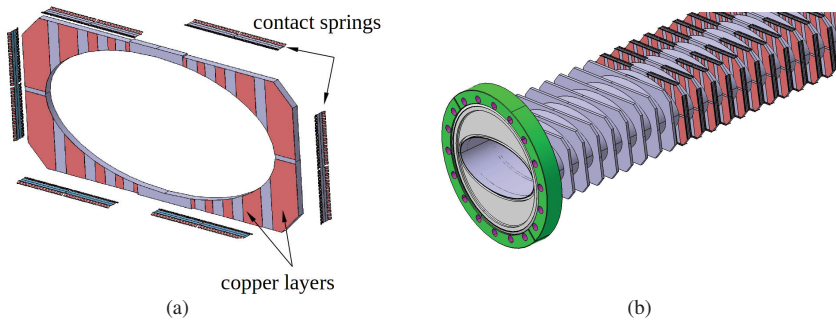


Fig. 2. (a) The strength rib adapted for the contact cooling, (b) the vacuum chamber with a contact cooling. The copper paths are giving in red.

2. Analytical calculations

2.1. Dynamic power losses in the vacuum chamber of the first full size prototype dipole for the SIS100

According to the design the vacuum chamber of the first prototype magnet is cooled by a cooling circuit build of the four cooling tubes which are electrically connected to the chamber via the ribs (see Fig. 1). This approach allows to keep the temperature of the vacuum chamber on the required level of < 15 K [2], nevertheless the cooling circuit acts as a closed electrical loop. In the interaction with a time-varying magnetic field it causes eddy currents which disturb the homogeneity of the magnetic field in the aperture of the magnet. The eddy currents and dynamic power losses were calculated analytically for the different parts of the vacuum chamber [5]. The induced current density j is given by

$$j(z) = \sigma E_z = \sigma \dot{B} x, \quad (1)$$

with σ the electrical conductivity, \dot{B} the time varying magnetic field and E the electric field strength. The dissipated power P_{ind} is given by

$$\frac{P_{ind}}{l} = \sigma d \dot{B}^2 \int_{v.c.} x^2 ds, \quad (2)$$

where d is the thickness of the chamber wall and l its length. The dynamic power losses in the elliptic beam pipe can be calculated from Eq. (2) by transformation from Cartesian coordinates to the polar coordinate system. For an ellipse one gets $x = a \cos \phi$, $y = b \sin \phi$ and Eq. (2) can be written as

$$\frac{P_{ell}}{l} = \sigma d a^3 \dot{B}^2 \int_0^{2\pi} \cos^2 \phi \sqrt{\sin^2 \phi + \epsilon^2 \cos^2 \phi} d\phi. \quad (3)$$

The dynamic power losses in the cooling circuit can be calculated as

$$\frac{P_{tube}}{l} = \sigma \dot{B}^2 \delta^2 A_{tube} \quad (4)$$

where A_{tube} correspond to the cross-section area of the cooling tube and δ is half of the distance between the cooling tubes. The main design parameters of the vacuum chamber as well as the calculated dynamic power losses are presented in the Table 1. One can see that the cooling circuit of the vacuum chamber generates

Parameter		Value	Dimension
<i>elliptic beam tube</i>			
thickness	d	0.3	mm
major half axis	a	64.6	mm
minor half axis	b	29.6	mm
length	l	2969.0	mm
<i>cooling tube</i>			
half of the distance between the cooling tubes	δ	57.25	mm
cross-section	A_{tube}	15.7	mm ²
dynamic power losses in the elliptic tube	P_{ell}	13.96	W
dynamic power losses in the cooling tubes	$P_{\Sigma tube}$	16.96	W
total losses	P	30.91	W

Table 1. The main design parameters of the of the vacuum chamber and dynamic power losses estimated by analytical calculations

power losses which are comparable to the losses in the elliptical beam pipe. The eddy currents and power losses in the other loops, formed by rib and cooling tubes, were detailed discussed in the [5]. The calculated results agree well with the results obtained by FEM (Finite element method) simulations and with the values measured on the first full size prototype magnet which amounts to 32.14 W, see [6].

The magnetic field within the aperture of the magnet was calculated using a short 3D model simulated in ANSYS (FEM based engineering simulation software). The data on a reference ellipse with semi-major axis $a = 57.5$ mm and semi-minor axis $b = 30.0$ mm were extracted from the grid. Out of these data elliptic and circular multipoles were calculated [7]. These plane circular multipoles describe a complex field $\mathbf{B} = B_y + iB_x$ by

$$B_y + iB_x = \sum_{n=1}^{\infty} \mathbf{C}_n \left(\frac{\mathbf{z}}{R_{ref}} \right)^{n-1} \quad (5)$$

with the coefficients $\mathbf{C}_n = B_n + iA_n$, $\mathbf{z} = x + iy$, and R_{ref} - the reference radius (40 mm within this text). Here n denotes the order of the multipole component, where $n = 1$ corresponds to the dipole and $n = 2$ to the quadrupole component of the field. To get an impression of the field homogeneity one uses dimensionless relative multipoles \mathbf{c}_n

$$b_n + ia_n = \mathbf{c}_n = \frac{\mathbf{C}_n}{\mathbf{C}_m} 10^4, \quad (6)$$

with \mathbf{C}_m the desired multipole of the magnet, particularly for a dipole magnet it is B_1 . The size of the relative multipole is given in units with 1 unit = 100 ppm. Fig. 3 gives the relative sextupole and decapole

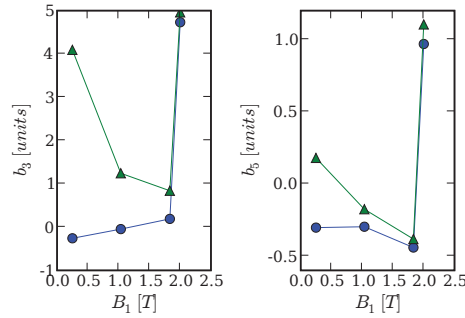


Fig. 3. Field deterioration in the aperture of the magnet based on the current vacuum chamber design. The sextupole $-b_3$ and decapole- b_5 component of the field. The blue lines denote the static field, the green lines represent the dynamic field for a ramp rate of 4 T/s.

component of the magnetic field obtained from the simulations. One can see that in the transient mode the field within the vacuum chamber is significantly disturbed by the eddy currents, see also [5].

To reduce the field deterioration and to simplify the cooling layout of the machine a new design for the vacuum chamber was suggested and analysed.

2.2. Dynamic power losses in the vacuum chamber with a contact cooling

The previous FEM simulations showed that the vacuum chamber can be cooled by the yoke if a proper contact is warranted between the cold iron yoke of the magnet and the vacuum chamber [8]. A thermal path from the vacuum chamber to the cold yoke can be realised via the ribs coated with a thin copper strips and contact springs welded to the ribs, (see Fig. 2). In this case the additional cooling circuit, sources of large eddy currents, can be removed and thus field inhomogeneity and losses are not required any more. Furthermore this approach significantly simplify the cryogenic layout of the machine.

In the first step the eddy currents and thus caused power losses in the copper layers were calculated for different values of thickness and width of the layers using Eq.(2). The total dynamic power losses in the copper strips are given in the Fig. 4(a). Next the heat transfer capacity via the copper strips was analysed. The heat transfer from the vacuum chamber surface to the yoke consists of the following parts

- the heat conduction from the beam pipe over the copper layers to the springs
- the contact resistance of the springs themselves.

The first one can be calculated while the second one can only be safely established by measurements, see section. 3.

Selecting the thickness of the copper layer one has to trade off between the required heat conduction power per Kelvin and the acceptable eddy currents. The conduction power P_i of the i^{th} strip is given by

$$P_i = \frac{a_i d_i \Delta T \bar{\lambda}}{b_i} \quad \text{with} \quad \bar{\lambda} = \frac{1}{\Delta T} \int_{T_{yoke}}^{T_{v.c.}} \lambda(T) dT \quad (7)$$

with a_i the width, b_i the height and d_i the thickness of the copper strip, ΔT the temperature difference between magnet yoke and chamber, and λ is the specific thermal conductivity for the appropriate temperature range. The magnet's yoke temperature T_{yoke} is assumed to be 5 K [8] while the target temperature of the vacuum chamber is set to be 5 K - 10 K higher than the yoke's temperature, depending on the region on the chamber surface. One can see in the Fig. 4(b) that already a 50 μm thick layer with a width of 5 mm will provide a heat transfer power of about 240 W for a temperature gradient of 5 K. This is roughly eight times the power dissipated in the vacuum chamber and should be already sufficient. So for the heat transport one only needs to consider the temperature of the yoke and the contact resistance of the springs to the yoke.

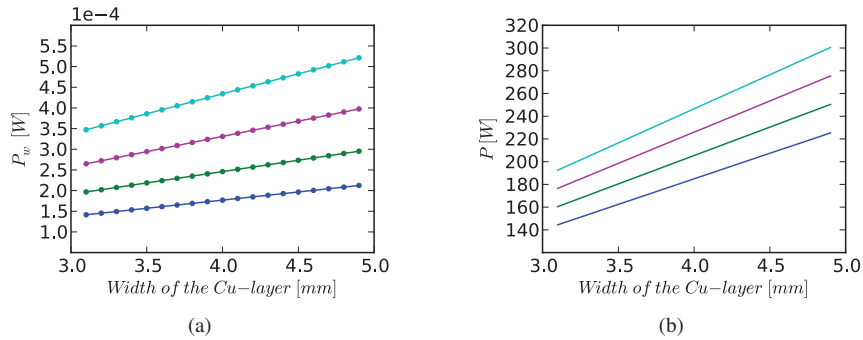


Fig. 4. Results of the analytical calculations for the vacuum chamber with a contact cooling. (a) Heat dissipated in the Cu layers due to eddy currents for different thicknesses of the Cu layer, (b) heat transport via the Cu layers between the chamber and the yoke versus the thickness a_i of the layer. Blue lines - 45 μm , green lines - 50 μm , magenta lines - 55 μm , cyan lines - 60 μm .

2.3. Mechanical stability

An efficient cooling via the heat conduction can be provided in vacuum, assumed in the magnet cryostat during an operation, only by the reliable mechanical contact between the cold yoke and the vacuum chamber. Some simulation were done to analyse the behaviour of the magnet assembly during the cool-down and the ramping to analyse the mechanical contact between the magnet yoke and the contact springs of the vacuum chamber, (see Fig. 5). The simulation results show that the proposed design guarantees a stable contact between the yoke and the contact springs during the magnet operation.

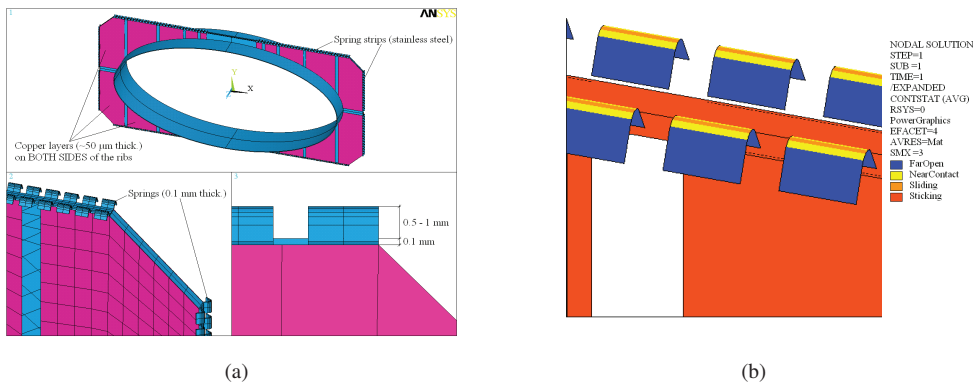


Fig. 5. ANSYS simulations. (a) Short 3D model for the alternative design of the vacuum chamber with a contact springs on the rib's edges, (b) Status of the contact springs during the ramping.

3. Model measurements

The contact resistance between the yoke and the vacuum chamber is a critical property which has to be revised by measurement on a mock-up (see Fig. 6)(a). For the mock-up a segment of the present vacuum chamber was used. So-called "thermal conductive" ribs with contact springs made of 0.1 mm thick stainless steel foil were coated with a 25 μm layer of pure silver. The cooling pipes were removed and the "thermal" ribs were fixed to the stiffness ribs. Further, a ohmic heater was added next to a simple coil, allowing to simulate the eddy current heating during magnet operation. The measurements on the mock-up will start during this month at the test facility at GSI.

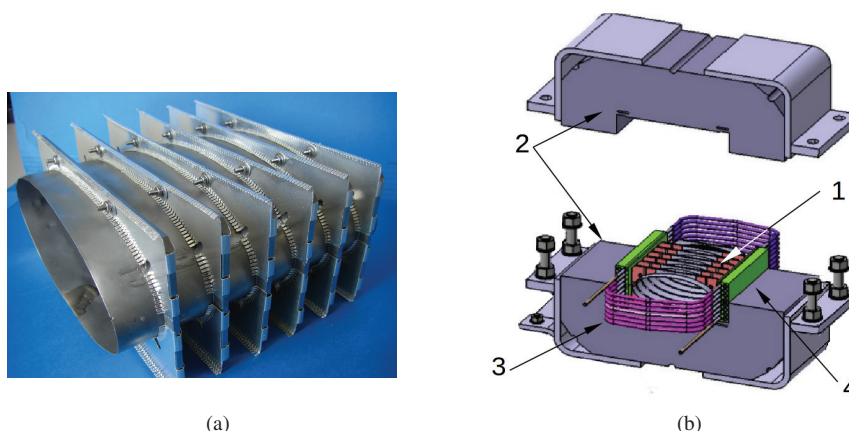


Fig. 6. The vacuum chamber with a direct cooling. Test set-up. (a) Segment of the vacuum chamber. (b) Mock-up assembly for the test: 1 segment of the vacuum chamber with "thermal conductive" ribs, 2 yoke segments, 3 cooling circuit of the coil, 4 segment of the superconducting coil.

4. Conclusion

The vacuum chamber is a critical hardware component of an ion accelerator and has to fulfil many different antagonistic requirements. The proposed solution, cooling the vacuum chamber via the cold yoke, defines the position of the vacuum chamber accurately and simplifies the cooling scheme of the accelerator.

The heat conduction path between the heat source, the eddy currents within the vacuum chamber, and the heat sink, the magnet yoke, can be shorted by small strips of copper. Calculations show that thin copper layers of $50\text{ }\mu\text{m}$ provide a heat transfer of approx 240W if a proper thermal contact is assumed at temperature difference of 5 K to 10 K. Therefore this approach seems to be feasible.

The remaining open question is the contact resistance between the yoke and springs attached to the ribs, which can only be obtained by a measurement. A first test on a mockup is being prepared and will be tested during this year.

References

- [1] Fischer E. *et al.* Supercon. SIS100 prototype magnets design, test results IEEE. T. Appl. Supercon, to be published.
- [2] Fischer, E., Mierau A., Schnizer P., Macavei J., Wilfert S., Spiller P. SIS100 Fast ramped magnets and their cryopump functionality for the operation with high intensity intermediate charge state heavy ions. IPAC'10, May ,2010,
- [3] Fischer E.*et al.* Numerical Analysis of the Operation Parameters of Fast Cycling Superconducting Magnets. Applied Superconductivity Conference ASC08, ser.IEEE Trans. On Appl. Supercon. vol. 19, no 3, June 2009, pp. 1266-1267.
- [4] Fischer E., Macavei J., and Mierau A. GSI MT Internal Note: MT-INT-EF-2009-001, October 2009.
- [5] Fischer E. *et al.* Impact of the beam pipe design on the operation parameters of the superconducting magnets for the SIS100 synchrotron of the FAIR project. EUCAS09, September 2009.
- [6] Fischer E. *et al.* Fast Ramped Superferric Prototype Magnets of the FAIR Project, First Test Results and Design Update. PAC 09, Vancouver , May 2009.
- [7] Schnizer, P., Schnizer B., Akishin P., Fischer E.. Theory and application of plane elliptic multipoles for static magnetic fields. In NIMA v. 607, num. 3, pp. 505 - 516, 2009.
- [8] Fischer E., Kurnishov R., and Shcherbakov P. Analysis of coupled electromagnetic-thermal effects in superconducting accelerator magnets. In EUCAS07, Edinburgh, Scotland 2007
- [9] Fischer E. *et al.* In WAMSDO Workshop, pp. 147–156. CERN, January 2009.